Tectonophysics 530–531 (2012) 80–86

Contents lists available at SciVerse ScienceDirect

Tectonophysics

journal homepage: www.elsevier.com/locate/tecto

Global pattern of earthquakes and seismic energy distributions: Insights for the mechanisms of plate tectonics

P. Varga [a], F. Krumm [b], F. Riguzzi [c,*], C. Doglioni [d], B. Süle [a], K. Wang [b], G.F. Panza [e]

[a] Geodetic and Geophysical Research Institute, Seismological Observatory, Hungary
[b] Geodätisches Institut, Universität Stuttgart, Germany
[c] Istituto Nazionale di Geofisica e Vulcanologia, Roma, Italy
[d] Dipartimento di Scienze della Terra, Università Sapienza, Roma, Italy
[e] Dipartimento di Geoscienze, Università di Trieste, and ICTP SAND group, Italy

ARTICLE INFO

Article history:
Received 1 July 2011
Received in revised form 12 October 2011
Accepted 14 October 2011
Available online 23 October 2011

Keywords:
Global seismicity
Declustered catalogue
Earthquake energy distribution
Plate tectonics

ABSTRACT

In this paper, we analyse the distributions of number of events (N) and seismic energy (E) on the Earth's surface and along its radius as obtained from the global declustered catalogue of large independent events ($M \geq 7.0$), dissipating about 95% of the Earth's elastic budget. The latitude distribution of the seismic event density is almost symmetric with respect to the equator and the seismic energy flux distribution is bimodal; both have their medians near the equator so that they are equally distributed in the two hemispheres. This symmetry with respect to the equator suggests that the Earth's rotational dynamics contributes to modulate the long-term tectonic processes.
The distributions of number and energy of earthquakes versus depth are not uniform as well: 76% of the total earthquakes dissipates about 60% of the total energy in the first ~50 km; only 6% of events dissipates about 20% of the total amount of energy in a narrow depth interval, at the lower boundary of the upper mantle (550–680 km). Therefore, only the remaining 20% of energy is released along most of the depth extent of subduction zones (50–550 km). Since the energetic release along slabs is a minor fraction of the total seismic budget, the role of the slab pull appears as ancillary, if any, in driving plate tectonics. Moreover the concentration of seismic release in the not yet subducted lithosphere suggests that the force moving the plates acts on the uppermost lithosphere and contemporaneously all over the Earth's outer shell, again supporting a rotational/tidal modulation.

1. Introduction

One of the most significant physical characteristics of earthquakes is the energy they radiate that may have a great impact on mankind. The study of the energy dissipated by large seismic events and its distribution may provide insights on the acting dynamics. A significant amount of papers, based on the analysis of complete catalogues containing all-size events (independent and aftershocks) above a threshold magnitude, has analysed the latitudinal distribution of the numbers of events, N, and their energy, E (e.g. Chouhan and Das, 1971; Denis et al., 2002; Levin and Chirkov, 2001; Levin and Sasorova, 2009; Riguzzi et al., 2010; Shanker et al., 2001; Sun, 1992; Varga, 1995). All these papers evidence that no significant seismic activity exists beyond latitudes $\pm 65°$ N and the distribution of the released seismic energy is zonal, with a maximum at the equator and two others near latitudes $\pm 45°$ N.

Many other papers have investigated the origin of deep earthquakes, the physical mechanism able to release elastic energy at great depths and the distributions of N and E (Abe and Kanamori, 1979; Chouhan and Das, 1971; Gutenberg and Richter, 1936, 1938, 1942, 1954, 1956; Kirby et al., 1991; Richter, 1979, and reference therein). Independently from the causes generating earthquakes at great depths, they all agree that the distributions of N and E are not uniform along the Earth radius. According to Frohlich (2006) only 25% of all earthquakes have focal depths exceeding 60 km and following Abe and Kanamori (1979) only about 0.2% of energy is released by deep focus earthquakes (depths larger than 300 km). Below the upper mantle (at about 680 km depth) the Earth becomes silent and deformations occur in the viscous regime. Such analyses are based on complete catalogues of all the events with $M \geq 7.0$, taking therefore into account all the largest aftershocks occurred in seismic sequences.

The goal of the present study is to investigate the distributions of N and E at the Earth surface and their depth dependence from a declustered catalogue to avoid possible biases introduced by the aftershocks, given that their number is relevant and their locations are driven by the master events. In fact, it is well known that the stress transfer produced by seismic events leads to changes in the probability of earthquake occurrence (Steacy et al., 2005). In other words, the distribution of mainshocks and related aftershocks cannot be considered a distribution of independent seismic events.

* Corresponding author. Tel.: +39 06 51860266.
E-mail address: federica.riguzzi@ingv.it (F. Riguzzi).

0040-1951/$ – see front matter © 2011 Elsevier B.V. All rights reserved.
doi:10.1016/j.tecto.2011.10.014

In this study, we have considered only large events (M≥7.0) just to manage a homogeneous and complete dataset (Romashkova, 2009), keeping in mind that about 95% of the total earthquake energy is released by such events.

2. The catalogue

The earthquake catalogues of 20th century can be considered statistically complete for events with M≥7.0 (Kossobokov, 2004; Pacheco and Sykes, 1992). Then, our study is based on the global catalogue of all M≥7.0 events recorded in 1900–2009, as a selection from the catalogue compiled by Shebalin (1992), extended with Preliminary Determination of Epicentres (PDE)-Monthly Listing (at the moment data for 2010 and 2011 are available as Weekly and Quick Epicenter Determinations), for a total amount of 2003 events. In this catalogue all the magnitude types are preserved, as reported in the original USGS/NEIC data. Thus, the catalogue is a multicolumn list containing the epoch of each event, the location and magnitudes (Mb, the average of a station body wave magnitude, Ms, the average of a station surface wave magnitude, and other authoritative magnitudes supplied with their types). The moment magnitude values, M_W, start to appear routinely in 1993, therefore they are not listed for most of the earthquakes in the 20th century, in particular for all mega-quakes. The elimination of possible duplicates and identification of aftershocks was obtained by Kossobokov and Romashkova from the complete catalogue by the "window method", as described in Keilis-Borok et al. (1980), the same method applied in the Global M8 test (Kossobokov et al., 1999). Other methods could be of course successfully employed (Van Stiphout et al., 2010).

In this way, 274 aftershocks with M≥7.0 have been removed from the initial complete catalogue. The declustered catalogue lists 1729 events from 1900 to 2011, frequently with more than one value of magnitude, most of them Ms. In particular, Ms is assigned to about 80% of the events, M_w to about 14% (since 1993 up to now) and M_b and M_L to the remaining 6%. To avoid major problems with magnitude heterogeneity (Pacheco and Sykes, 1992) and taking into account that hypocentral determinations are known with sufficient accuracy only since the middle of 20th century, in the following, only data from 1960 to 2011 are considered. Therefore, the initial catalogue is reduced from 1729 to 654 events (about 57% quantified by Ms and 43% by Mw).

In order to obtain uniform magnitude values, all the M_W have been transformed in M_S by applying the non-linear calibration curve reported by Utsu (2002). The M_S scale tends to saturation for $M_S \geq 8$ (Kanamori, 1983), so that energies for $M_S \geq 8$ could be underestimated. Nevertheless, all the initial Ms values have been depth corrected following the calibration procedure defined in Herak et al. (2001), since it is statistically proven that routine values of Ms of deep events are underestimated. These recalibrations improve significantly the relationship between M_S and the seismic moment Mo, limiting the problem of saturation and therefore of energy evaluation (Bormann and Saul, 2009), so that we can consider our recalibrated M larger than Ms, near to Mw.

3. Latitudinal and longitudinal distribution of *E* and *N*

The space–time distribution of earthquakes from 1960 to 2011 shows that polar areas are completely silent, in fact all the events occurred within latitudes 62°S–71° N; a clustering of the largest ones seems to occur after 1990, as can be seen in Fig. 1.

The analysis of distributions of *N* and *E* has been defined in latitude classes of 10°, applying a normalisation by spherical areas, thus obtaining N^* (earthquake density) and E^* (energy flux) (Fig. 2). Seismic energy should be considered very carefully due to problems induced by magnitude assessment, so that the subsequent considerations have a purely indicative aim (Kagan, 2003). From

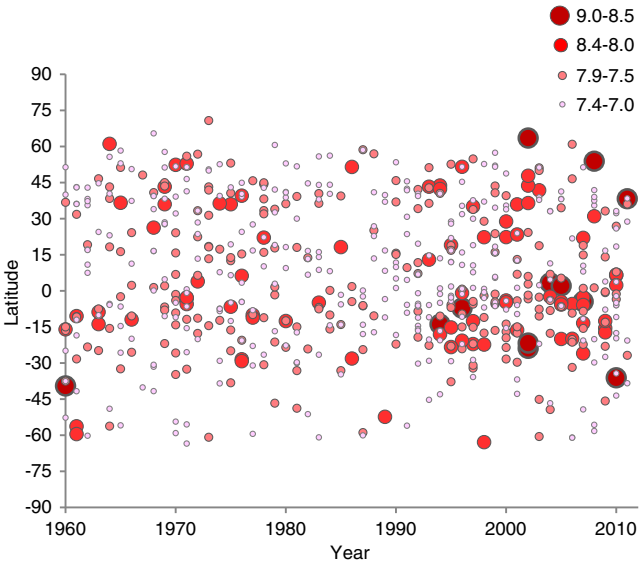

Fig. 1. Space-time distributions of the earthquakes listed in the declustered catalogue in the time interval 1960–2011. Bullet sizes according to different M classes.

Ms, energy can be computed by the classical Gutenberg relation (Gutenberg, 1956a, 1956b),

$$\mathrm{Log}_{10}E = 1.5 \cdot \mathrm{Ms} + 4.8\,(\mathrm{joule}).$$

Energy values are known with very low accuracy, in fact, if we optimistically accept a mean standard deviation on magnitudes of 0.23 (Giardini et al., 1997), from the error propagation law, the energy uncertainty may be evaluated as $\Delta E = 1.5 \cdot \ln(10) \cdot E \cdot \Delta M \sim 0.79 \cdot E$ (joule),

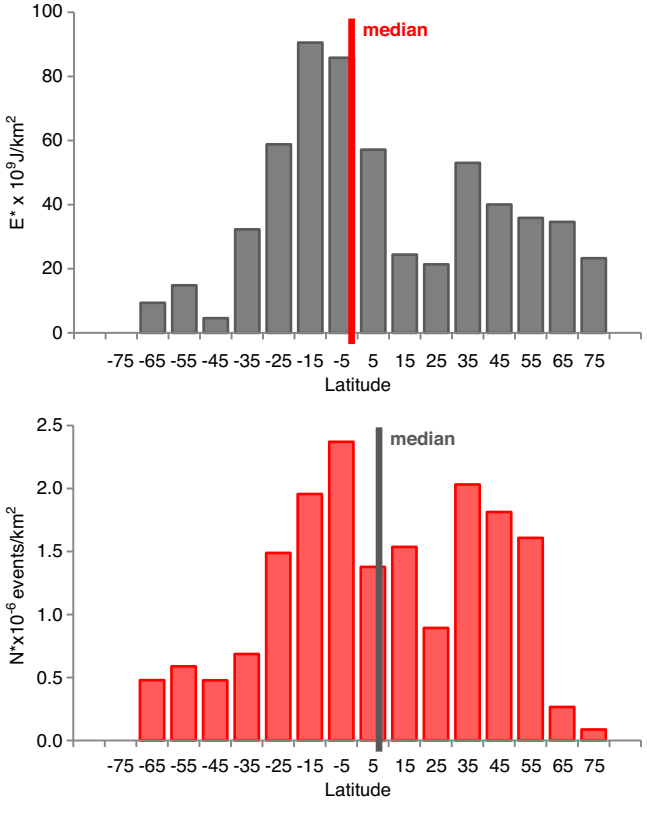

Fig. 2. Distribution of N^* (density of events) and E^* (energy flux) of the earthquakes with M≥7.0 along Earth's latitude for the time interval 1960–2011 (10°-sampling). The seismicity decreases towards the polar areas and has a maximum in the latitude range −10°–0°.

that can be considered a lower bound for energy accuracy. More recently, Kagan (2003) has re-evaluated the magnitude accuracy by testing different catalogues, obtaining an upper bound for the standard deviation of 0.275 that would increase the energy uncertainty to about 95%. The problem of magnitude accuracy could be overcome by using seismic moments of CMT catalogues (Convers and Newman, 2011); however, the short time span covered by these catalogues limits their statistical use.

Coming back to us, even if the minimum level of uncertainty at which seismic energy is known is about 80%, it is still worth using it since the interest is here mainly focused on giving the pattern of the distribution of E^* with latitude, rather than on single values of energy. Nevertheless, since the estimate of the energy E, based on the magnitude–energy relation, is greatly affected by the errors in magnitude, the number of events N is probably a more robust representation of the occurrence of moderate to large earthquakes than E (Kanamori, 1977).

In Fig. 2 are reported the distributions of N^* and E^* in 10° latitude classes of all the 654 events. Both the distributions are bimodal with maxima falling in the classes $-20° \le Lat \le -10°$ N and $-10° \le Lat \le 0°$ N, respectively. The median of $N^*$is at 8° N, while the median of E^* is at −2° N.

The latitudinal distributions show persistent features and result rather independent from magnitude values, i.e. not biassed by few exceptionally strong events and not significantly corrupted by magnitude saturation. In fact, similar patterns are obtained excluding all the events with $M > 8.0$ (Fig. 3), with maxima falling in the class $-10° \le Lat \le 0°$ N. In this case the medians overlap at the equator.

In contrast with what reported by some authors (e.g. Sun, 1992), the present analysis based on a declustered catalogue shows that the two hemispheres release the same amount of energy and without zonal symmetry of energy release, thus evidencing that the inclusion of aftershocks in the analysis is able to bias the distributions, in particular, when the number of earthquakes is considered as a proxy.

The persistent bimodal pattern of N^* and E^* with respect to the equatorial area seems to indicate a signature of the Earth's rotational dynamics on the occurrence of large seismic events. The same persistent bimodal pattern is found by analysing separately the distributions of the shallow (depths ≤ 100 km) and deep events (depths > 100 km), as shown in Fig. 4.

Similarly, the distribution of the number, N, and energy, E, of earthquakes with $M \ge 7.0$ in the time interval 1960–2011, along the Earth's longitude is shown in Fig. 5. This analysis may appear trivial, since the distribution of most of the seismicity simply follows the location of the world subduction zones. However, it helps to understand the latitudinal distribution of seismicity. Notice for example the low seismicity between −45° 45° E, involving the African and the western part of the Eurasian plates, as also well evident in Fig. 7 (central panel).

4. Depth distribution of seismicity

The depth distributions (50 km depth classes) of N and E retrieved by the declustered catalogue are shown in Fig. 6. N decreases with increasing depth as $\sim 1/h^2$ (h is the focal depth in km) up to about 300 km. From 300 to 500 km the events are sporadic, while below this depth they increase significantly up to 650 km. In particular, 90% of the events occurs within 300 km while the remaining 10% from 300 to 700 km; about 76% of the total amount of earthquakes is concentrated in the first depth class (0–50 km); 18% occur from 50 to 300 km and the remaining 6% up to 680 km. As far as energy is concerned, 80% is dissipated within 300 km, the remaining 20% from 300 to about 680 km, where most of the energy dissipation is viscous. About 60% of the total amount of energy is concentrated in the first depth range (0–50 km), with a sharp maximum ($\sim 1.2 \times 10^{19}$ J); 20% is dissipated from 50 to 300 km and the remaining 20% up to 680 km. Only the 6% of all the

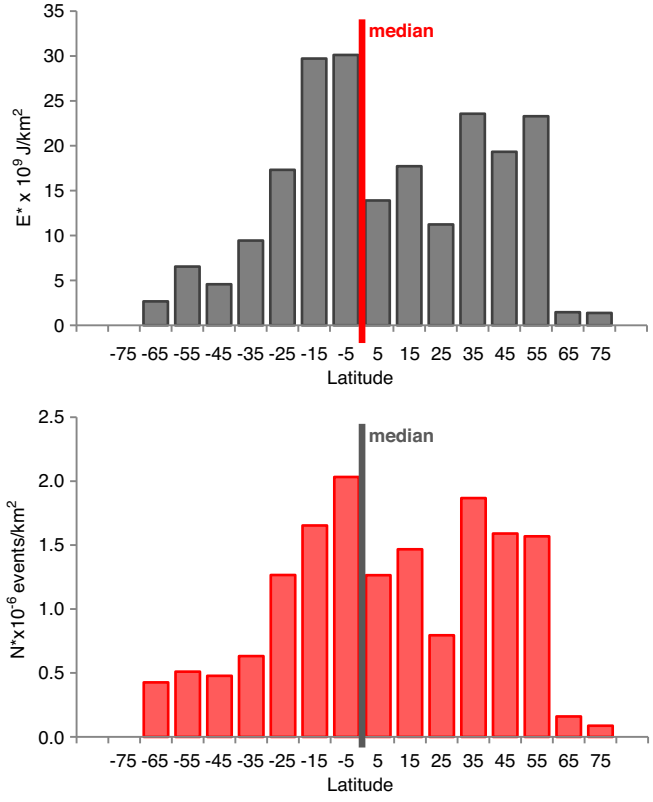

Fig. 3. Distribution of N^* (density of events) and E^* (energy flux) of the earthquakes with $8.0 > M \ge 7.0$ along Earth's latitude for the time interval 1960–2011 (10°-sampling). Even if all the events with $M > 8$ are excluded, the pattern shown in Fig. 2 is preserved. The maxima fall in the class $-10° \le Lat \le 0°$ N and the medians overlap the equator.

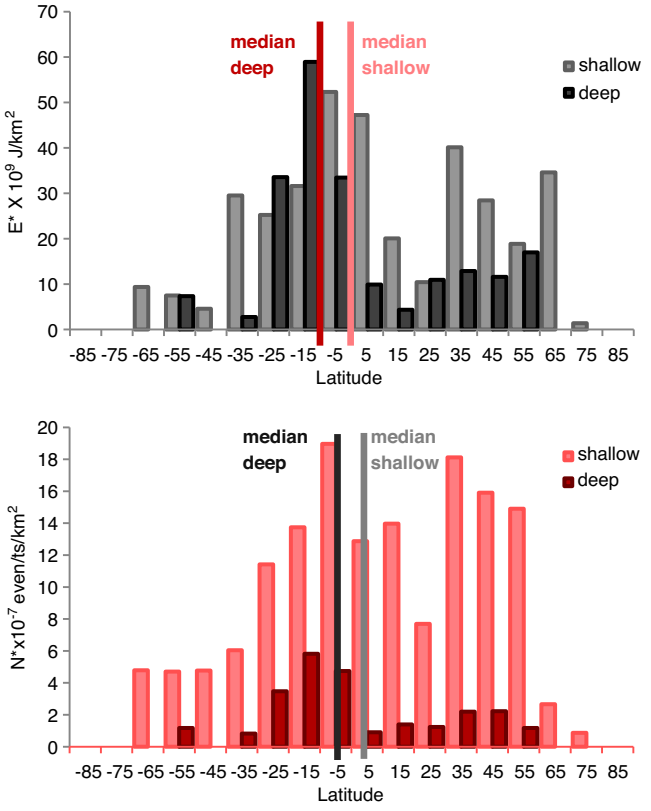

Fig. 4. Latitudinal distribution of N^* and E^* of earthquakes with $M \ge 7.0$ (10°-sampling), for shallow (<100 km) and deep (>100 km) events.

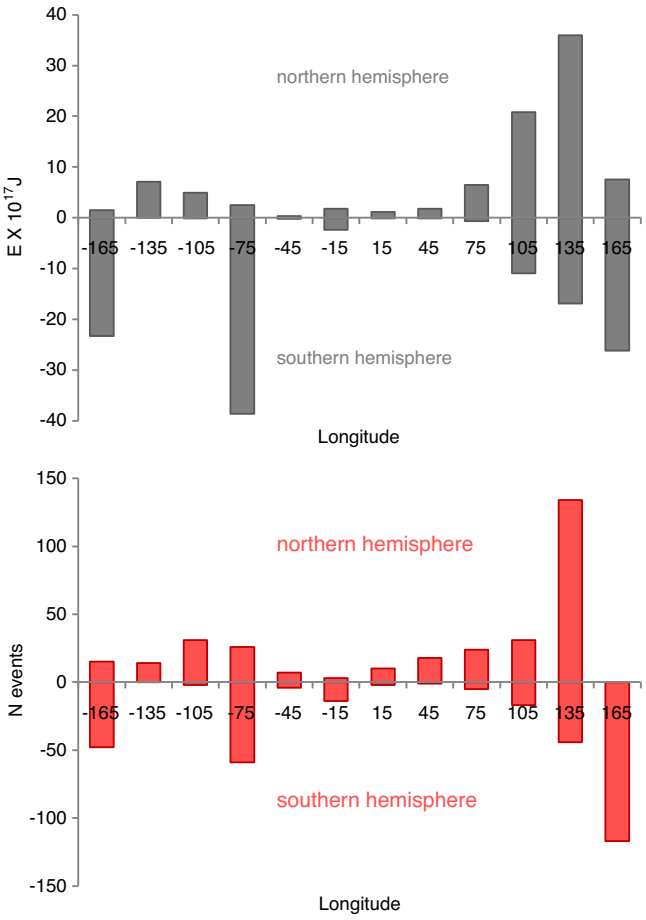

Fig. 5. Longitudinal distribution of *N* and *E* of earthquakes with M≥7.0 (10°-sampling). Each distributions is divided by hemisphere, so that negative values are an artefact just to represent *N* and *E* of the southern hemisphere. Most of the events are concentrated along subduction zones.

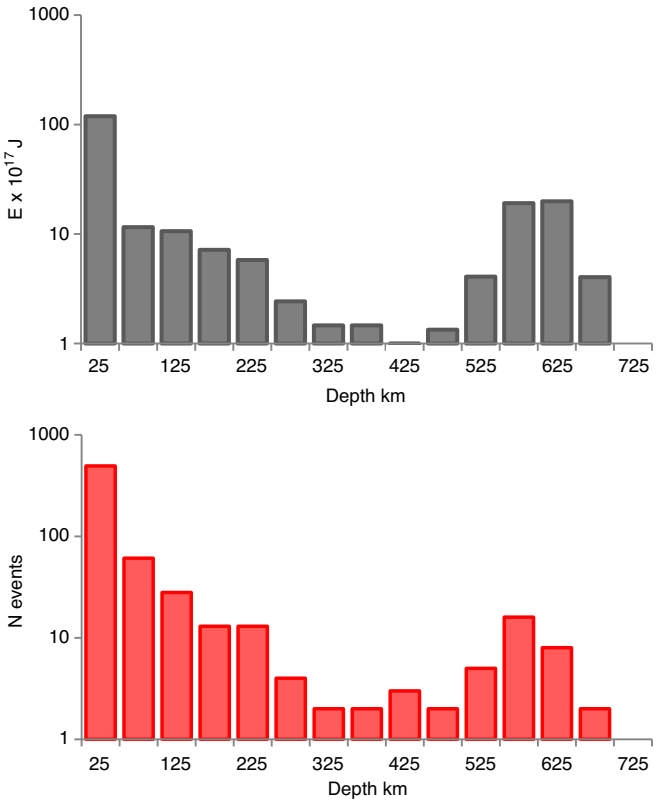

Fig. 6. Depth distribution of *N* and *E* of earthquakes with M≥7.0 (50 km-sampling). *N* and *E* axes in logarithmic scale. Most of events and seismic energy are restricted in the shallow lithosphere. Most of the residual elastic energy is radiated between 550 and 680 km of depth.

earthquakes release the 20% of the total amount of energy in the deep interval (550–680 km). The deep event clustering is marked by high energy release (energy peak ~4.7×10^{18} J).

Not all subduction zones characterised by high seismic energy radiation at shallow depth are connected to deep earthquake energy sources (Fig. 7). Mostly shallow focus earthquakes delineate the lithospheric slabs penetrating into the mantle in Central America, Barbados, Aleutians and east of New Zealand. On the other hand, the subduction zones of Japan, Kuriles and Kamchatka (Fig. 7A), of Kermadec Island area (Fig. 7B), of Pacific coast of South America between latitudes 10° S and 30° S (slabs in Peru-Bolivia and Chile, Fig. 7C) and of South Asia (Sumatra, Banda Sea and Timor, Philippine and East Luzon, Fig. 7D) are marked both by shallow and deep earthquake sources ($h\geq500$ km). Moreover, in the 300–550 km depth interval (e.g., Riguzzi et al., 2010), in the W- or SW-directed slabs *N* and *E* are larger than in the opposite E- or NE-directed slabs.

In the source areas where shallow and deep focus earthquakes occur, two angles can be identified: slab dip β taken from Riguzzi et al. (2010) and the angle α between the surface and the straight line connecting shallow and deep source zones (average dip, Fig. 8). We find, in the case of the E-directed slabs of South America $\alpha=50°$, while the typical slab dip β in this region, for $h<70$ km, is $\beta=20°$ (Table 1). Similar values are observed in the Sumatra source zone (NE-directed slab). This means that typically $\alpha-\beta\approx30°$ and the Benioff–Wadati zones consisting of both shallow and deep source zones (Fig. 7C, D) are not straight and lead to infer three possible processes: (a) bending of the slab, (b) breaking of the slab and (c) the upward suction of the lower mantle (Doglioni et al., 2009). For the W-directed slabs the situation is different. In the Far East, Japan and Kuriles–Kamchatka source zones (Fig. 7A) and Kermadec Islands (Fig. 7B) we get smaller values for $\alpha-\beta$, averaging at about 6°, even when the α values are close to the case of the E-directed slabs. This means that the Benioff–Wadati zones are not bent in these cases. In other words, the deep seismicity along W- or SW-directed slabs is regularly connected to the superficial part of the subduction zone ($\alpha-\beta\approx6°$), while along E- or NE-directed subduction zones the large difference between dips ($\alpha-\beta\approx30°$) rather suggests a different origin of the deep seismicity. In fact, along these subduction zones, the seismicity is very scarce between 300 and 550 km of depth (Riguzzi et al., 2010) and most of the elastic energy radiated by deep events is concentrated in the depth interval between 550 km and 680 km (Fig. 6), somewhat above the lower border of the transition zone given in PREM (Dziewonski and Anderson, 1981). Green (2007) proposed that deep earthquakes are related to shearing instabilities accompanying high-pressure phase transformations. A physical mechanism (transformational faulting) has been proposed for the generation of deep earthquakes (Kirby et al., 1991). However, contrary to the common assumption of the presence of a slab at such depths, it is possible to invoke mantle suction process and shear between upper and lower mantle generated by a sort of Venturi effect: the mantle, in correspondence of E- or NE-directed subduction zones, can flow through a surface that is significantly reduced, with respect to standard situations, by the subduction plate marked by seismicity not deeper than about 300 km. Therefore the deep earthquakes along the E- or NE-directed slabs may be related to the subduction system, which is sucking up the mantle, but they occur in the mantle without requiring the presence of any slab (e.g., Doglioni et al., 2009). In support of this hypothesis, most of the focal mechanisms of deep events (Harvard CMT Catalogues) have a major extensional component, well consistent with an accelerated mantle flow through narrow structures (e.g. Van der Hilst, 1995) across

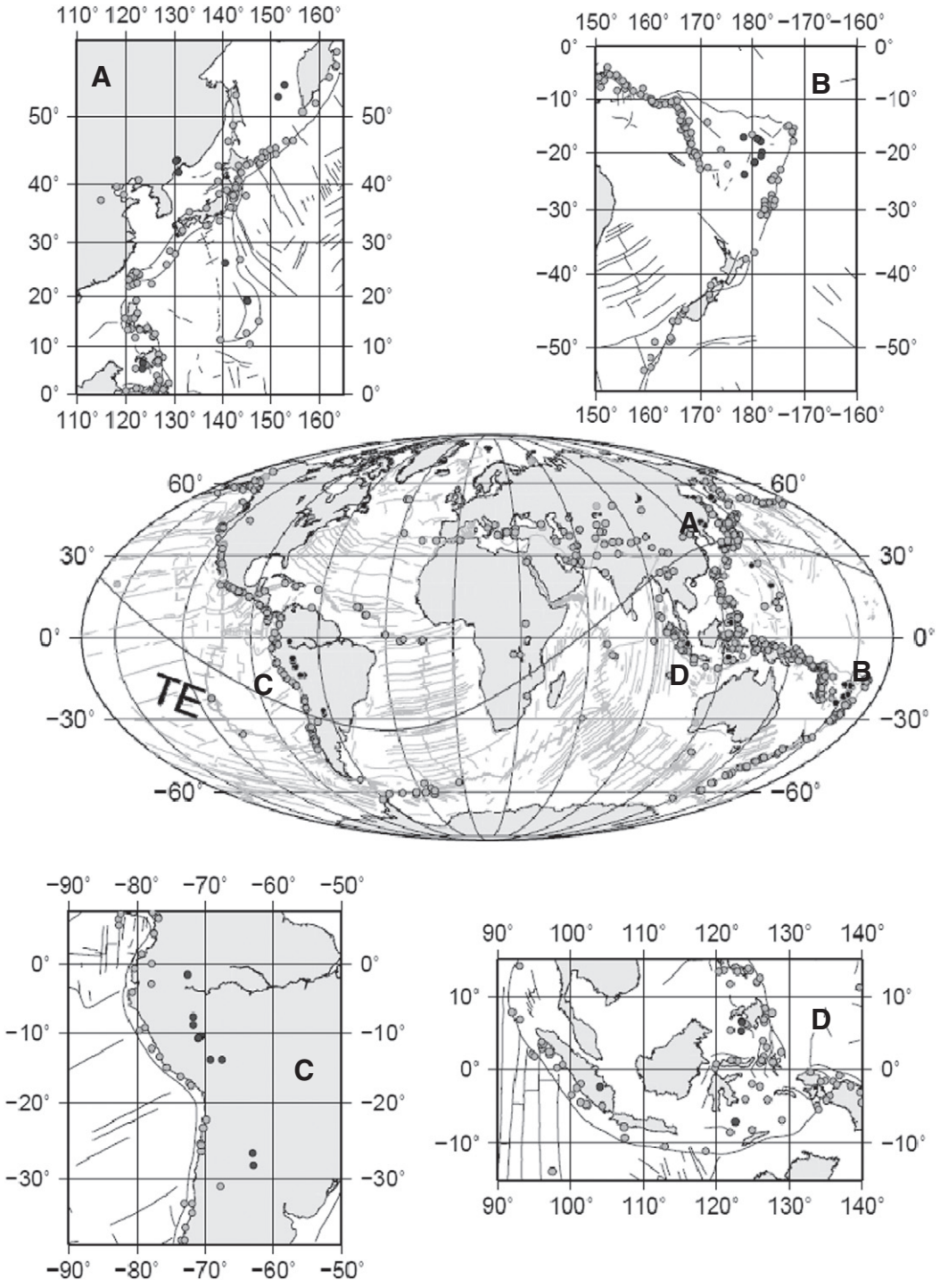

Fig. 7. Distribution of shallow (depth interval 0–50 km, grey bullets) and deep (depth interval 500–680 km, black bullets) focus earthquakes. A) Japan–Kuriles subduction zones; B) Kermadec–Tonga subduction zones; C) West South America (Peru and Chile subduction zones); D) Indonesia (Sumatra, Banda sea and East Luzon or Philippine subduction zones); TE – tectonic equator.

the lower boundary of the C layer, thus suggesting pressure reduction (Venturi effect).

5. Discussion and conclusions

With the purpose of evidencing robust and unbiased features, unlike previous reviews of the Earth's seismicity distribution (e.g., Stein and Wysession, 2003; Sun, 1992), this study is based on a declustered catalogue. The gross features evidenced by earlier studies, such as no relevant energy delivery in the polar areas and drastic decrease of earthquakes below 50 km of depth are nicely confirmed. In addition we note that the global regularities and the equatorial locations of the medians of all the distribution of *E* and *N* seem to be consistent with the Earth's rotational dynamics. On the other hand, a good correlation between long time series of energy, number of events and polar motion was first observed in Kanamori (1977) and recently reconsidered in Riguzzi et al. (2010).

The phenomenon, which could supply the appropriate mechanism capable to generate the required force, is the decrease of the axial rotation speed due to tidal friction, in agreement with Riguzzi et al.

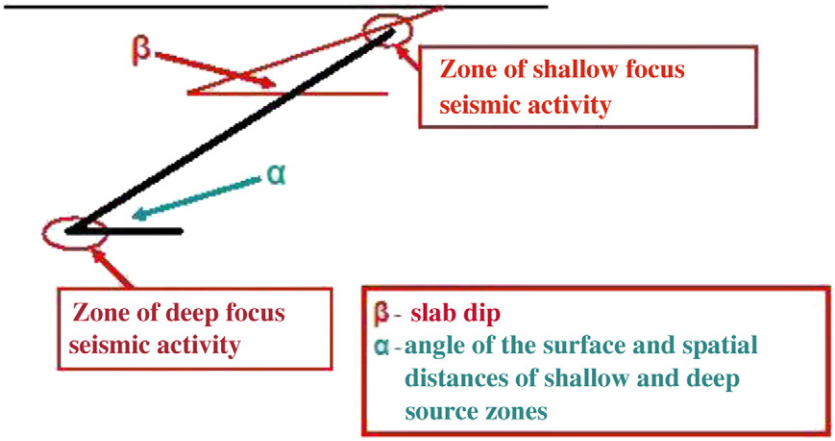

Fig. 8. When plotting the seismicity across a slab, the shallow part of it has an angle that may or may not correspond to the one connecting the shallow seismicity to the deeper events. The sketch shows the shallow slab average dip, β, while the angle α is the angle between the shallow seismicity and the deep source zones. Along E–NE-directed subduction zones, where a seismic gap is generally present between 300 and 500 km, the two angles differ substantially, whereas they are not so different along W-directed slabs (see Table 1).

(2010) who formulated the hypothesis that a significant portion of despinning energy, due to tidal friction, is converted into tectonic energy.

The relaxation of an equatorial bulge due to the slowing of rotation of a planetary body has been invoked as a mechanism generating differential stresses between the equatorial and polar areas (Amalvict and Legros, 1993; Melosh, 1977). However the despinning of the Earth is too slow to generate differential stresses comparable to those observed along present plate boundaries (e.g., Parsons, 2006). Moreover, unlike other planets of the solar system, the Earth is marked by plate tectonics. In absence of it, other minor forces can be relevant in determining deformation and faulting of a static crust or lithosphere.

The frequency of earthquakes predicted by the Gutenberg–Richter law, proven to be valid for large events only at global scale (Molchan et al., 1997), supports the existence of a force acting and dissipating energy all over the entire Earth's lithosphere; the existence of coherent global scale intermediate-term tectonic processes in the lithosphere and the occurrence of the global scale seismic premonitory patterns of impending mega-earthquake (Romashkova, 2009) are all consistent with the results of the present study.

The stress orientation over the Earth lithosphere is determined by the shape, distribution, tectonic type of plate boundaries and direction of plates motion (e.g., Zoback, 1992) and the accumulation of stress, the magnitude of the stress tensors and the differential stress are quite proportional to the relative velocity among plates (e.g., Scholz, 2003; Stein and Wysession, 2003). Therefore we expect greater earthquakes at fast converging zones (Ruff and Kanamori, 1980); this correlation appears weak, but it becomes rather robust when the recurrence rate is considered (Gutscher and Westbrook, 2009). In the equatorial belt of the Earth, plates move faster (Bird et al., 2009), and this is consistent with the largest seismic energy dissipation along the same area; on the contrary the relative plate velocities tend to decrease towards the polar areas, and seismicity consequently decreases.

According to Kirby et al. (1996) and Venkataraman and Kanamori (2004) the intra-slab seismicity is restricted to the cold cores of the slabs. However, as mentioned before, not all the subduction zones characterised by large seismic energy radiation at shallow depth are connected to deep earthquake energy sources (Fig. 7). Moreover, E- or NE-directed slabs have a major seismic gap between 250 and 550 km of depth. The comparison of the distribution of the shallow seismicity with that of the deep events indicates that the energy dissipation is concentrated in the shallow lithosphere mainly at low latitudes; on the contrary, the distributions of the number of earthquakes (deep and shallow) are bimodal with a predominant occurrence of low latitude deep events (Figs. 4 and 7).

Intraslab seismicity is mostly in down-dip compression along W- or SW-directed slabs, whereas it is more frequently a down-dip extension along the opposite E- or NE-directed slabs (Doglioni et al., 2007). These global scale asymmetries of subduction zones associated to those observed along oceanic ridges (Panza et al., 2010) can be envisaged as evidence of the net-rotation of the lithosphere which is moving westerly relative to the underlying mantle along a main path modelled by the so-called tectonic equator (TE), the great circle along which plates move faster (Crespi et al., 2007). The distribution of earthquakes in classes of distance with respect to the tectonic equator (TE), obtained by

Table 1
Slab dip, β, and average dip, α, the angle between the surface and the straight line connecting shallow and deep source zones. Notice the difference in the angles of the first three subduction zones, which are "E–NE-directed" (see text), whereas the remaining are W-directed and the two angles mostly coincide.

Subduction zones with deep earthquake activity	α°	β°
Peru	49	15
Chile	54	23
Sumatra	60	32
Banda Sea (Timor)	74	55
Philippine (East Luzon)	66	63
Japan	42	35
Kuriles–Kamchatka	45	45
Kermadec Islands	55	58

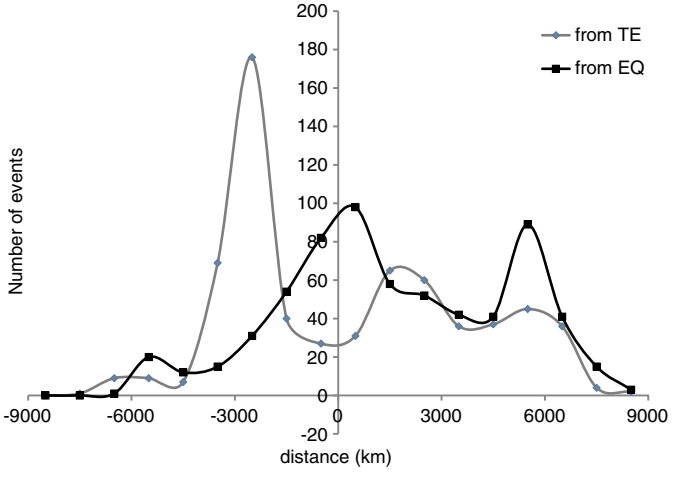

Fig. 9. Plot of N with respect to the distance of each event from the geographic equator (EQ), black line, and the tectonic equator (TE, Crespi et al., 2007), grey line.

rotating the Cartesian geocentric axes such that Z (the axis of Earth's rotation) is aligned to the net rotation axis of the lithosphere, shows minimum values near the TE. On the contrary, a maximum is found if earthquakes are grouped in classes of distance with respect to the equator (Fig. 9). This is the striking evidence that along the TE to a faster plate motion corresponds a relative minimum of seismic activity (0 distance, grey line).

The depth distribution of energy has two peaks: the most important (~60% of the seismic energy) is released by the shallow brittle crust (~30 km); the other is situated at the lower boundary of the transition zone between upper and lower mantle (responsible for ~20% of E). This fact indicates that the negative buoyancy of the slabs (slab pull) might not be the driving force of plates, due to the very limited amount of elastic energy dissipated within most of the slab volume (between about 50 and 520 km of depth). In the depth interval from about 520 km to 630 km, below the E- or NE-directed subduction zones the mantle is forced to flow through a surface that is significantly reduced, with respect to standard situations, by the subduction plate marked by seismicity, as a rule, not deeper than about 350 km. As a consequence there is reduction in fluid pressure (Venturi effect), well consistent with the extensional character of the focal mechanism of the deep earthquakes with $M \geq 7$ that occur there possibly even in absence of a broken sunken slab.

In conclusion, our study is consistent with a model in which the lithosphere and mantle form a chaotic self-organised system, where seismic energy appears generated and tuned by the combination of internal viscous mantle convection and rotational dynamics acting contemporaneously all over the lithosphere.

Acknowledgements

We are extremely grateful to L. Romashkova and V. Kossobokov for making available their seismic event catalogue and for their assistance in its use. This paper was partly completed in the framework of the bilateral project DFG-HAS 189 ("Study of the time dependent geophysical and geodetic processes"). Financial support from the MIUR COFIN 2008 is acknowledged.

References

Abe, K., Kanamori, H., 1979. Temporal variation of the activity of intermediate and deep focus earthquakes. Journal of Geophysical Research 84, 3589–3595.
Amalvict, M., Legros, H., 1993. Stresses in the lithosphere induced by the Earth rotation. In: Teisseyre, R. (Ed.), Physics and Evolution of the Earth's Interior, Volume 6: Dynamics of the Earth's Evolution. PWN Warszawa and Elsevier, Amsterdam, pp. 348–349.
Bird, P., Kagan, Y.Y., Jackson, D.D., Shoenberg, F.P., Werner, M.J., 2009. Linear and nonlinear relations between relative plate velocity and seismicity. Bulletin of the Seismological Society of America 99 (6), 3097–3113.
Bormann, P., Saul, J., 2009. Earthquake magnitude. In: Meyers, R.A. (Ed.), Encyclopedia on Complexity and Systems Science. Springer, Heidelberg.
Chouhan, R.K.S., Das, U.C., 1971. Preliminary report on global seismicity-frequency energy distribution of earthquakes. Pure and Applied Geophysics 89 (1), 98–108.
Convers, J.A., Newman, A.V., 2011. Global evaluation of large earthquake energy from 1997 through mid-2010. Journal of Geophysical Research 116, B08304. doi:10.1029/2010JB007928.
Crespi, M., Cuffaro, M., Doglioni, C., Giannone, F., Riguzzi, F., 2007. Space geodesy validation of the global lithospheric flow. Geophysical Journal International 168, 491–506. doi:10.1111/j.1365-246X.2006.03226.
Denis, C., Schreider, A.A., Varga, P., Závoti, J., 2002. Despinning of the Earth rotation in the geological past and geomagnetic paleointensities. Journal of Geodynamics 34 (5), 97–115.
Doglioni, C., Carminati, E., Cuffaro, M., Scrocca, D., 2007. Subduction kinematics and dynamic constraints. Earth-Science Reviews 83, 125–175. doi:10.1016/j.earscirev.2007.04.001.
Doglioni, C., Tonarini, S., Innocenti, F., 2009. Mantle wedge asymmetries along opposite subduction zones. Lithos 113, 179–189. doi:10.1016/j.lithos.2009.01.012.
Dziewonski, A.M., Anderson, D.L., 1981. Preliminary reference Earth model. PEPI 25, 297–356.
Frohlich, C., 2006. Deep Earthquakes. Cambridge University Press.
Giardini, D., Di Donato, M., Boschi, E., 1997. Calibration of magnitude scales for earthquakes of the Mediterranean. Journal of Seismology 1, 161–180.
Green, H.W., 2007. Shearing instabilities accompanying high-pressure phase transformations and the mechanics of deep earthquakes. Proceedings of the National Academy of Sciences of the United States of America. doi:10.1073/pnas.0608045104.
Gutenberg, B., 1956a. The energy of earthquakes. Quarterly Journal of the Geological Society of London 112, 1–14.
Gutenberg, B., 1956b. Great earthquakes 1896–1903. Eos Trans. AGU 37, 608–614.
Gutenberg, B., Richter, C.F., 1936. Materials for the study of deep-focus earthquakes. Bulletin of the Seismological Society of America 26 (4), 341–390.
Gutenberg, B., Richter, C.F., 1938. Depth and geographical distribution of deep-focus earthquakes. GSA Bulletin 49 (1), 249–288.
Gutenberg, B., Richter, C.F., 1942. Earthquake magnitude, intensity, energy, and acceleration. Bulletin of the Seismological Society of America 32, 163–191.
Gutenberg, B., Richter, C.F., 1954. Seismicity of the Earth, 2nd edition. Princeton University Press.
Gutenberg, B., Richter, C.F., 1956. Earthquake magnitude, intensity, energy and acceleration (second paper). Bulletin of the Seismological Society of America 46, 105–145.
Gutscher, M.-A., Westbrook, G.K., 2009. Great earthquakes in slow-subduction, low-taper margins. In: Lallemand, S., Funiciello, F. (Eds.), Subduction Zone Geodynamics. : Frontiers in Earth Sciences. Springer-Verlag Berlin Heidelberg, pp. 119–133. doi:10.1007/978-3-540-87974-9.
Herak, M., Panza, G.F., Costa, G., 2001. Theoretical and observed depth correction for M_S. Pure and Applied Geophysics 158, 1517–1530.
Kagan, Y.Y., 2003. Accuracy of modern global earthquake catalogs. PEPI 135, 173–209.
Kanamori, H., 1977. The energy release in great earthquakes. Journal of Geophysical Research 82 (20), 2981–2987.
Kanamori, H., 1983. Magnitude scale and quantification of earthquakes. Tectonophysics 93 (3–4), 185–199.
Keilis-Borok, V.I., Knopoff, L., Rotwain, I.M., 1980. Burst of aftershocks, long-term precursors of strong earthquakes. Nature 283 (5744), 259–263.
Kirby, S.H., Durham, W.B., Stern, L.A., 1991. Mantle phase changes and deep-earthquake faulting in subducting lithosphere. Science 252, 216–225.
Kirby, S.H., Stein, S., Okal, E.A., Rubie, D.C., 1996. Metastable mantle phase transformations and deep earthquakes in subducting oceanic lithosphere. Reviews of Geophysics 34 (2), 261–306.
Kossobokov, V.G., 2004. Earthquake prediction: basics, achievements, perspectives. Acta Geod. Geophys. Hung. 39 (2–3), 205–221.
Kossobokov, V.G., Romashkova, L.L., Keilis-Borok, V.I., Healy, J.H., 1999. Testing earthquake prediction algorithms: statistically significant advance prediction of the largest earthquakes in the Circum-Pacific, 1992–1997. Physics of the Earth and Planetary Interiors 111, 187–196.
Levin, B.W., Chirkov, Ye.B., 2001. Planetary maxima of the earth seismicity. Physics and Chemistry of the Earth, Part C 26 (10–12), 781–786.
Levin, B.W., Sasorova, E.V., 2009. Latitudinal distribution of earthquakes in the Andes and its Peculiarity. Advances in Geosciences 22, 139–145.
Melosh, H.J., 1977. Global tectonics of a despun planet. Icarus 31, 221–243.
Molchan, G., Kronrod, T., Panza, G.F., 1997. Multi-scale seismicity model for seismic risk. B.S.S.A. 87, 1220–1229.
Pacheco, J.F., Sykes, L.R., 1992. Seismic moment catalog of large shallow earthquakes, 1900 to 1989. BSSA 82 (3), 1306–1349.
Panza, G., Doglioni, C., Levshin, A., 2010. Asymmetric ocean basins. Geology 38 (1), 59–62.
Parsons, T., 2006. Tectonic stressing in California modeled from GPS observations. Journal of Geophysical Research 111, B03407.
Richter, F.M., 1979. Focal mechanisms and seismic energy release of deep and intermediate earthquakes in the Tonga–Kermadec region and their bearing on the depth extent of mantle flow. Journal of Geophysical Research 84 (B12), 6783–6795.
Riguzzi, F., Panza, G., Varga, P., Doglioni, C., 2010. Can Earth's rotation and tidal despinning drive plate tectonics? Tectonophysics 484 (1–4), 60–73.
Romashkova, L.L., 2009. Global-scale analysis of seismic activity prior to 2004 Sumatra-Andaman mega-earthquake. Tectonophysics 470, 329–344.
Ruff, L., Kanamori, H., 1980. Seismicity and the subduction process. Physics of the Earth and Planetary Interiors 23, 240–252.
Scholz, C.H., 2003. The Mechanics of Earthquakes and Faulting. Cambridge Univ. Press.
Shanker, D., Kapur, N., Singh, V.P., 2001. On the spatio temporal distribution of global seismicity and rotation of the Earth — a review. Acta Geod. Geophys. Hung. 36 (2), 175–187.
Shebalin, P.N., 1992. Automatic duplicate identification in set of earthquake catalogs merged together. U.S. Geol. Surv. Open-File Report 92–401 Appendix II.
Steacy, S., Gomberg, J., Cocco, M., 2005. Introduction to special section: stress transfer, earthquake triggering, and time-dependent seismic hazard. Journal of Geophysical Research 110, B05S01. doi:10.1029/2005JB003692.
Stein, S., Wysession, M., 2003. Introduction to Seismology, Earthquakes and Earth Structure. Blackwell Publishing.
Sun, W., 1992. Seismic energy distribution in latitude and a possible tidal stress explanation. Physics of the Earth and Planetary Interiors 71 (3–4), 205–216.
Utsu, T., 2002. Relationships between magnitude scales. In: Lee, W.H.K., Kanamori, H., Jennings, P.C., Kisslinger, C. (Eds.), International Handbook of Earthquake and Engineering Seismology, Part A. Academic Press, Amsterdam, pp. 733–746.
Van der Hilst, R.D., 1995. Complex morphology of subducted lithosphere in the mantle beneath the Tonga trench. Nature 374, 154–157.
Van Stiphout, T., Zhuang, J., Marsan, D., 2010. Seismicity Declustering, Community Online Resource for Statistical Seismicity AnalysisAvailable at http://www.corssa.org2010.
Varga, P., 1995. Temporal variation of the figure of the Earth and seismic energy release. Publication of the Institute of Geodesy and Navigation, University FAF, Munich, pp. 118–127.
Venkataraman, A., Kanamori, H., 2004. Observational constraints on the fracture energy of subduction zone earthquakes. Journal of Geophysical Research 109, B05302. doi:10.1029/2003JB002549.
Zoback, M.L., 1992. First- and second-order patterns of stress in the lithosphere: the World Stress Map Project. Journal of Geophysical Research 97 (B8), 11703–11728.